Supplementary Information for

Northern Scandinavian Mountains Supported by a Low-grade Eclogitic Crustal Keel

Metin Kahraman, Hans Thybo, Irina M. Artemieva, Alexey Shulgin, Peter Hedin, Rolf Mjelde

Correspondence to: h.thybo@gmail.com

This file includes:

Supplementary Figure 1.	Resolution test for the velocity model.
Supplementary Figures 2 - 4.	Ray coverage, traveltime fit and seismic sections with reduction velocity 8 km s^{-1} for three stacked airgun sources.
Supplementary Figures 5 - 9.	Ray coverage, traveltime fit and seismic sections with reduction velocity 8 km s^{-1} all five land shots.
Supplementary Figure 10.	Ray coverage for PmP and Pn phases, which defines Moho depth and sub-Moho velocity.
Supplementary Figure 11.	Ray coverage for Pn phases, which defines Moho depth and sub-Moho velocity with constant 8.2 km s^{-1} sub-Moho P velocity.
Supplementary Figure 12.	Ray coverage for PmP and Pn phases, which defines 7^{o} dip Moho.
Explanatory Note:	Gravity Model Sensitivity Test
Supplementary Figures 13 - 16.	Gravity model sensitivity test for upper mantle density variations.
Supplementary Figures 17 - 18.	Gravity model sensitivity test for compensation depth at 110 and 130 km, respectively.
Supplementary Table 1.	Seismic station parameters for data acquisition.
Supplementary Table 2.	Shot parameters for data acquisition.
Supplementary Table 3.	Statistical parameters of seismic P-wave modelling for all shots.
Supplementary Table 4.	Statistical parameters of seismic P-wave modelling for onshore explosive sources.

Supplementary Table 5. Statistical parameters of seismic P-wave modelling for airgun shots.

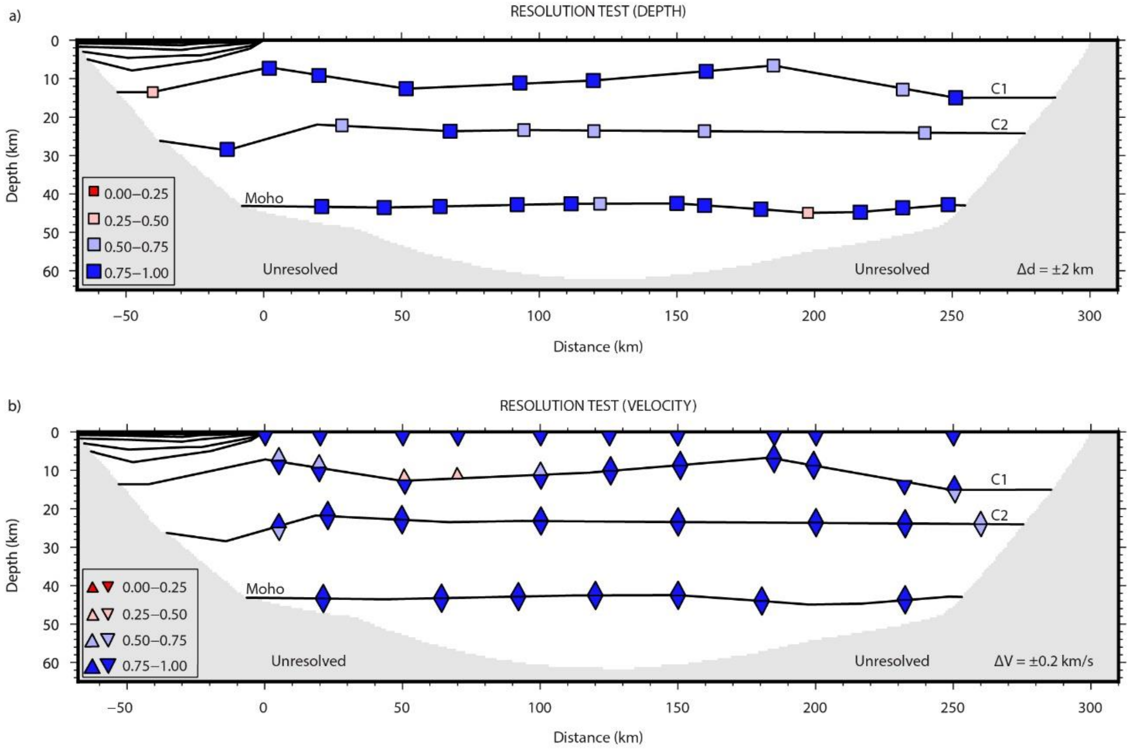

Supplementary Figure 1. Resolution test for the velocity model derived from the calculated diagonal values of the resolution matrix for depth and velocity. a) Resolution of depth to crustal discontinuities is generally high, in particular for the Moho depth. Depth uncertainty is $\Delta d = \pm 2$ km. **b)** Resolution of seismic P-wave velocity is generally high at all depth levels, including sub-Moho velocities. Velocity uncertainty is $\Delta V = \pm 0.2$ km s^{-1}.

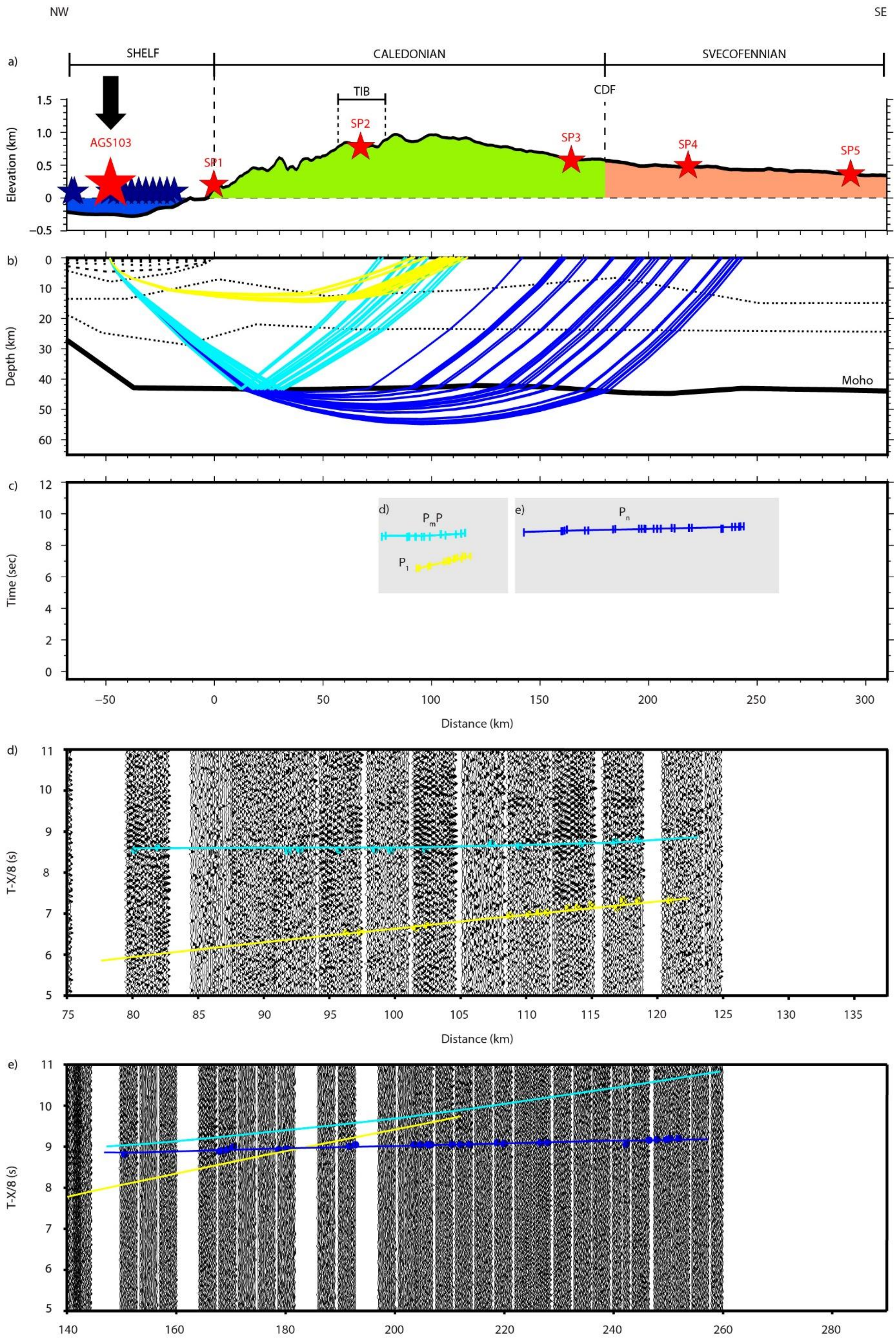

Supplementary Figure 2. Seismic travel time fit for airgun stack AGS103. a) Hypsometry with traversed geological units and locations of seismic sources: Red stars for onshore explosive sources SP1-5 and blue stars for offshore airgun stack locations AGS101-112, Large red offshore star shows location of AGS103. Abbreviations: CDF - Caledonian Deformation Front; TIB - Trans-Scandinavian Igneous Belt. **b)** Simplified P-wave velocity model with ray path coverage for AGS103. **c)** Travel time fit for AGS103 for model in Figure 2. Observed travel times are shown by vertical marks with length corresponding to uncertainty of picks, calculated arrival times are shown by solid lines. Abbreviations for seismic phases: P_1 – intra-crustal refraction, PmP – wide-angle reflection from Moho; Pn – refraction from below the seismic Moho. The seismic section is divided into two parts. **d and e)** Seismic sections with travel time picks for AGS103. Calculated arrival times are shown by lines with colour coding as in b and c.

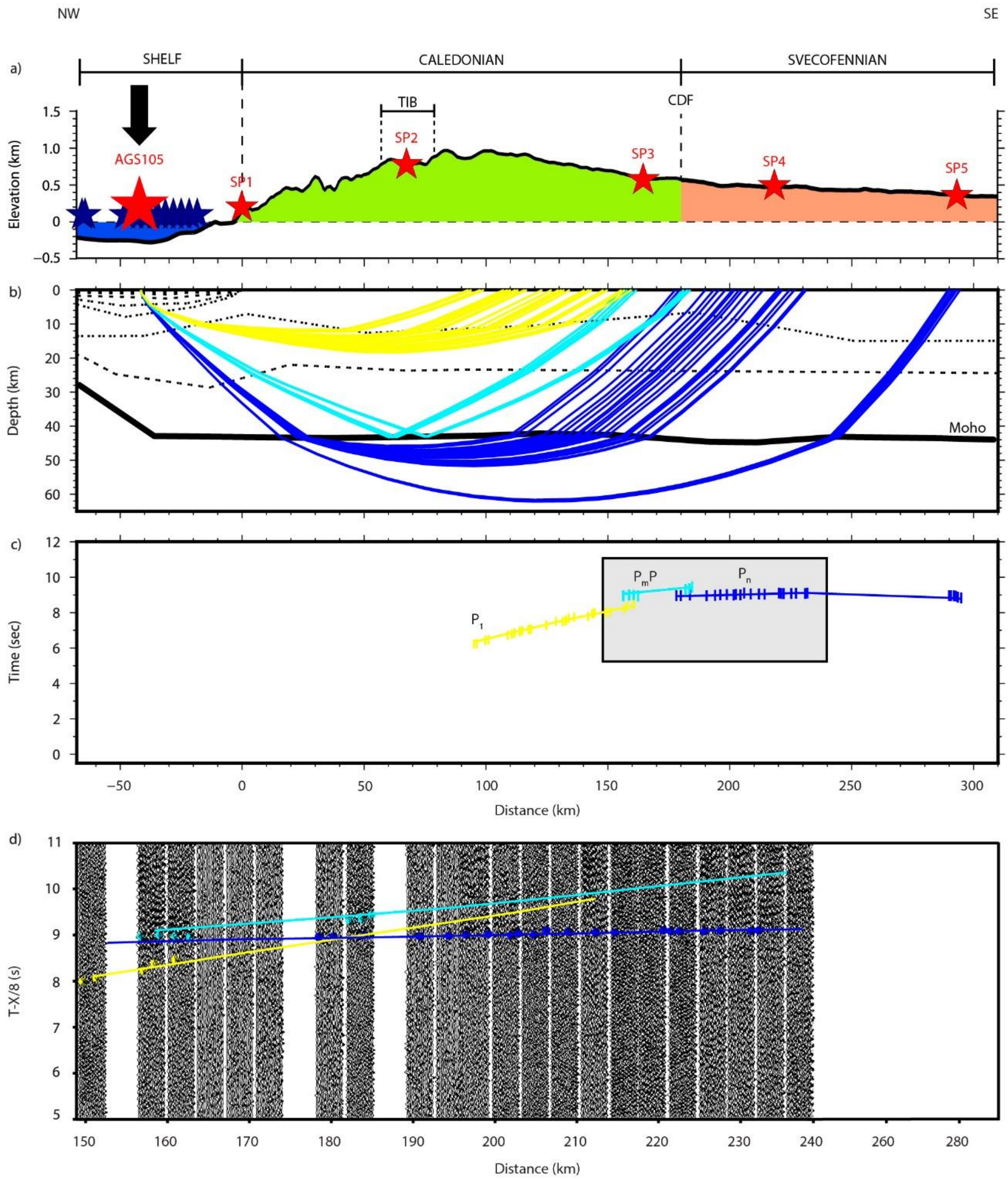

Supplementary Figure 3. Seismic travel time fit for airgun stack AGS105. As Supplementary Figure 2 for AGS105 instead of AGS103. The seismic section is presented in one part (d).

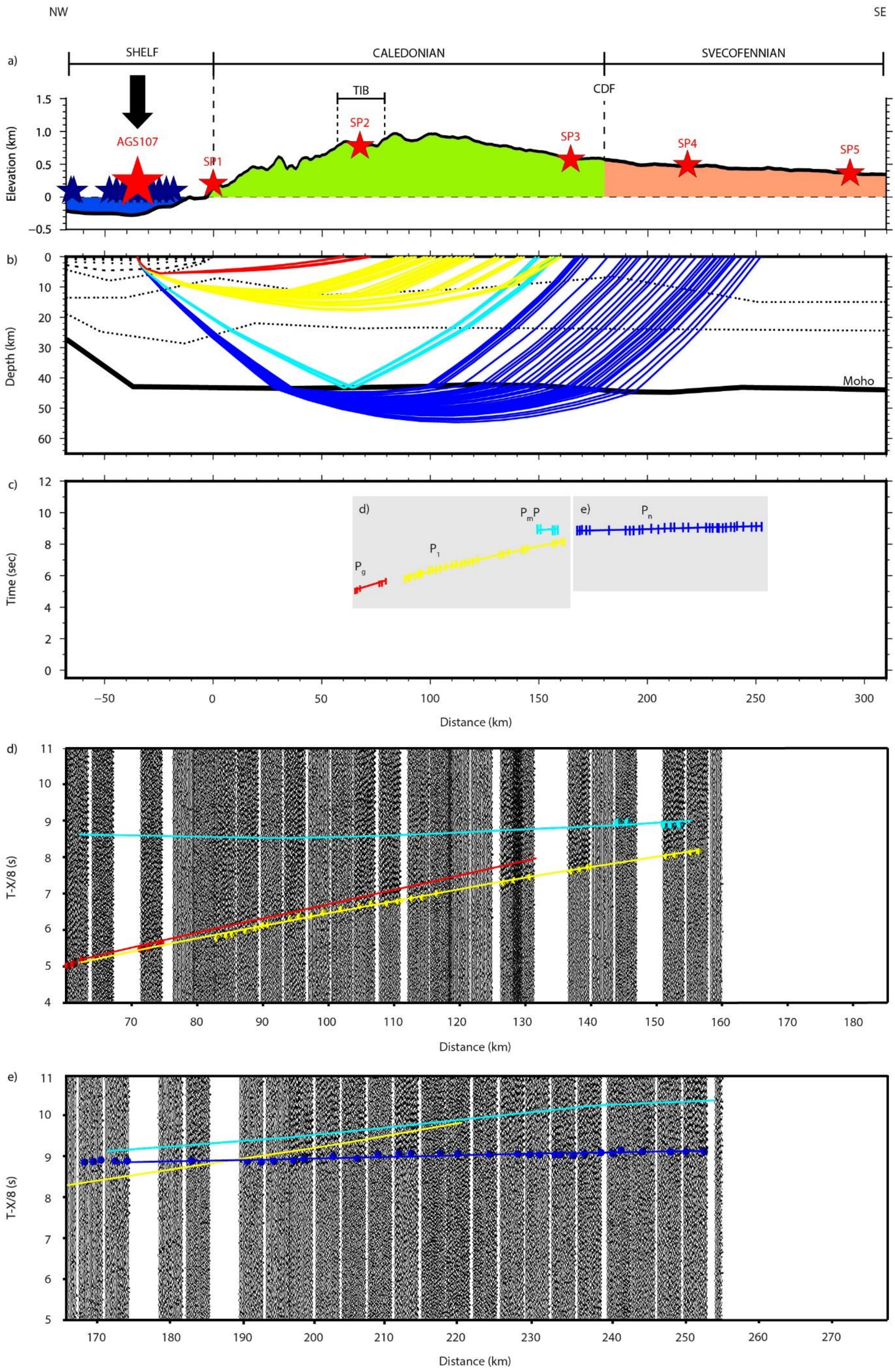

Supplementary Figure 4. Seismic travel time fit for airgun stack AGS107. As Supplementary Figure 2 for AGS107 instead of AGS103. The seismic section is divided into two parts. Additional abbreviation: P_g – Basement refraction. **d and e)** correspond to marked parts in c.

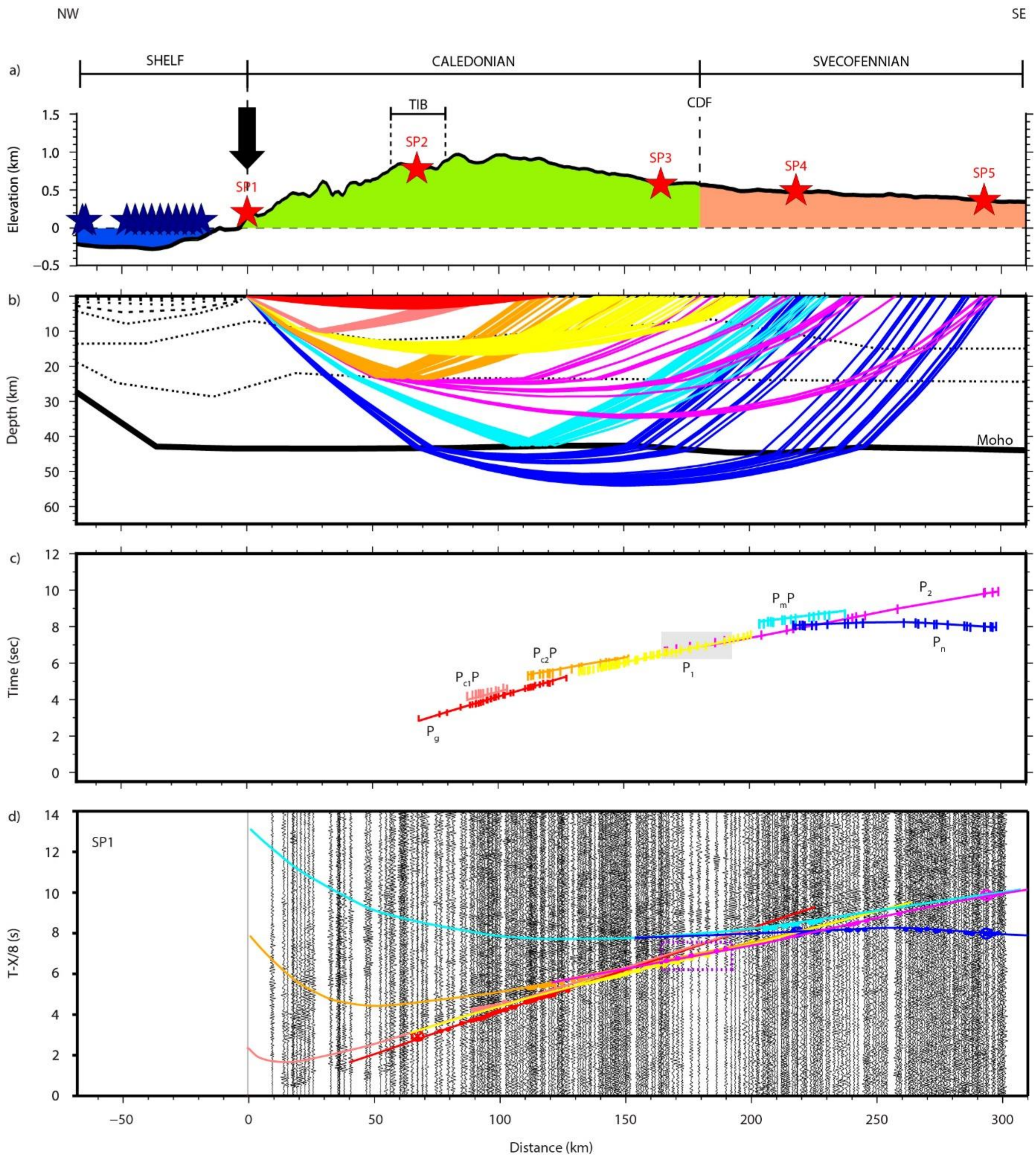

Supplementary Figure 5. Seismic travel time fit for SP1. As Supplementary Figure 3 for Sp1 instead of AGS107. Additional abbreviation: $P_{c1}P$ and $P_{c2}P$ - Intracrustal reflections. Light gray area in (c) and purple stipple regtangle in (d) are the are where P_1 and P_2 picked times where every other one may every other.

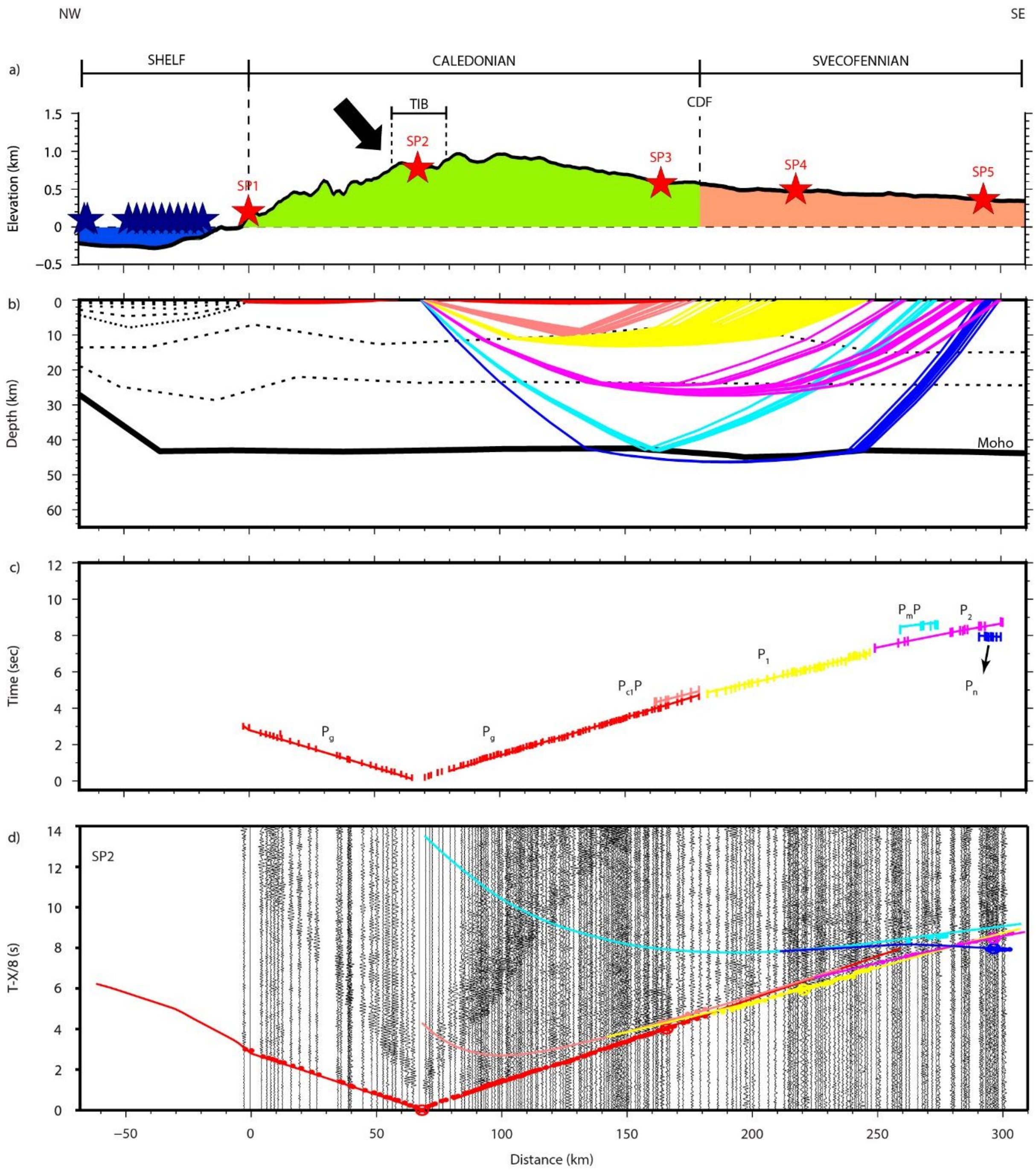

Supplementary Figure 6. Seismic travel time fit for SP2. As Supplementary Figure 4 for Sp2 instead of SP1.

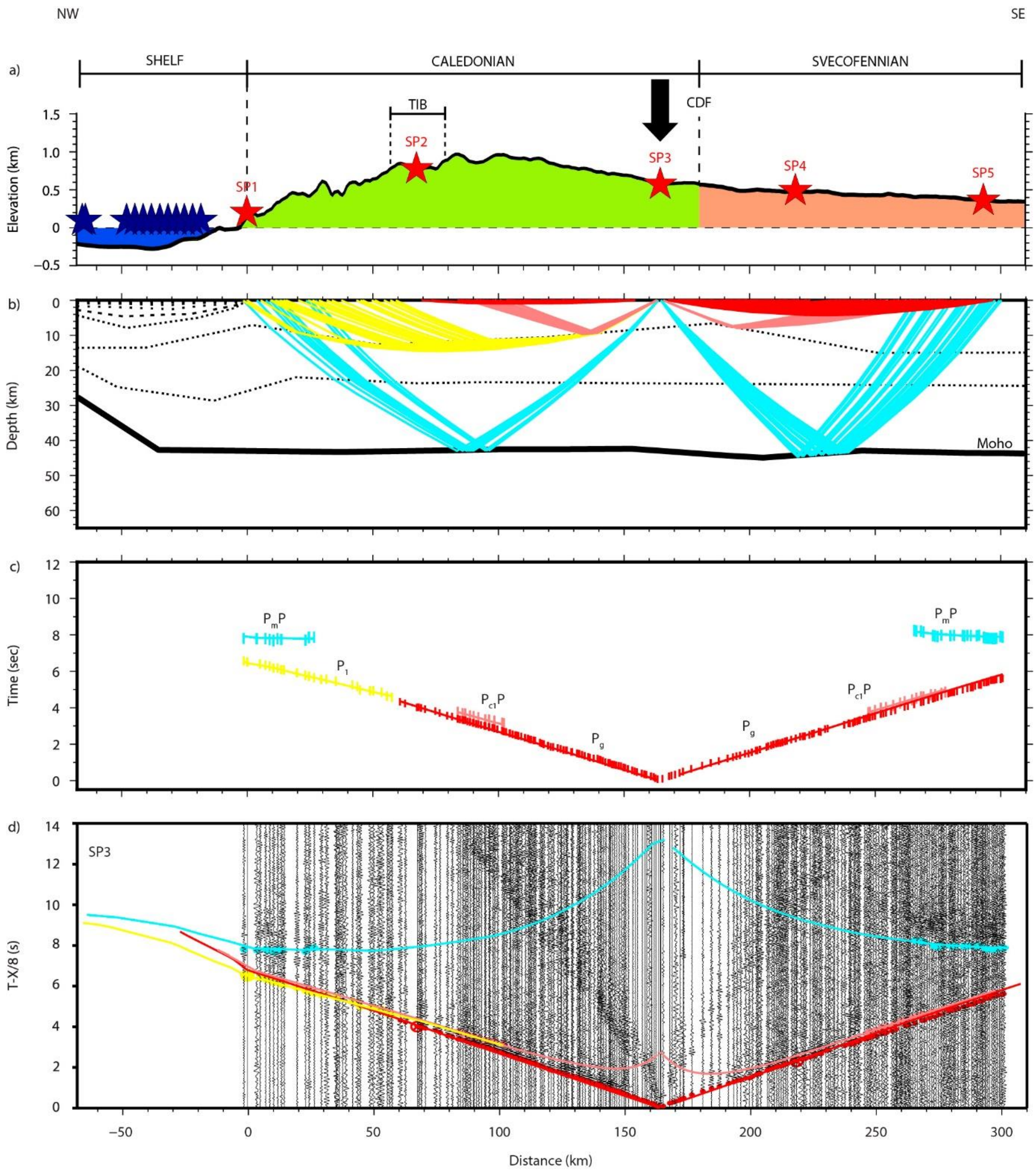

Supplementary Figure 7. Seismic travel time fit for SP3. As Supplementary Figure 4 for SP3 instead of SP1.

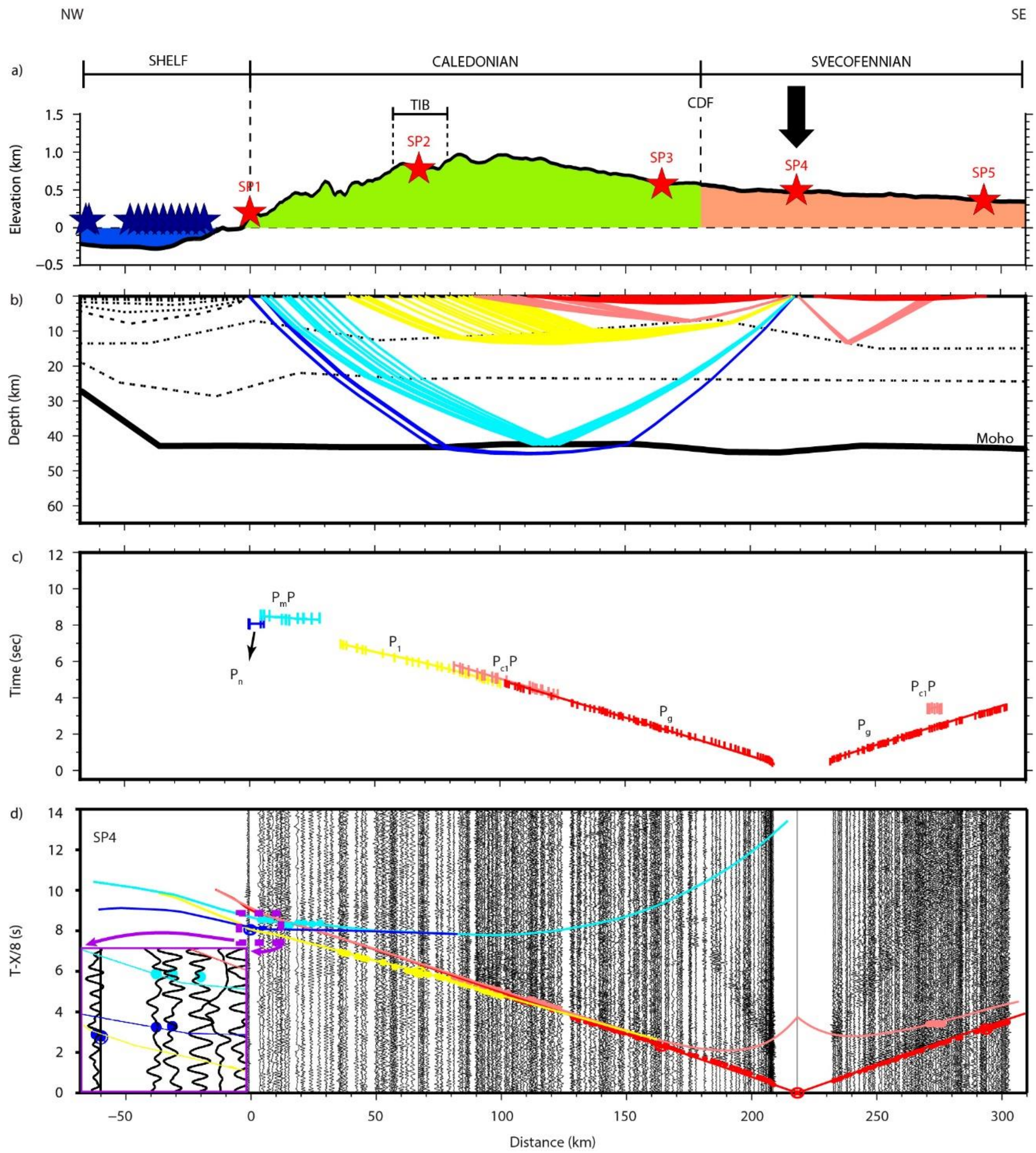

Supplementary Figure 8. Seismic travel time fit for SP4. As Supplementary Figure 4 for SP4 instead of SP1. Reciprocal arrival time for Pn is marked by purple cross with circle (d) and in zoomed display for enhancing resolution of the Pn phase.

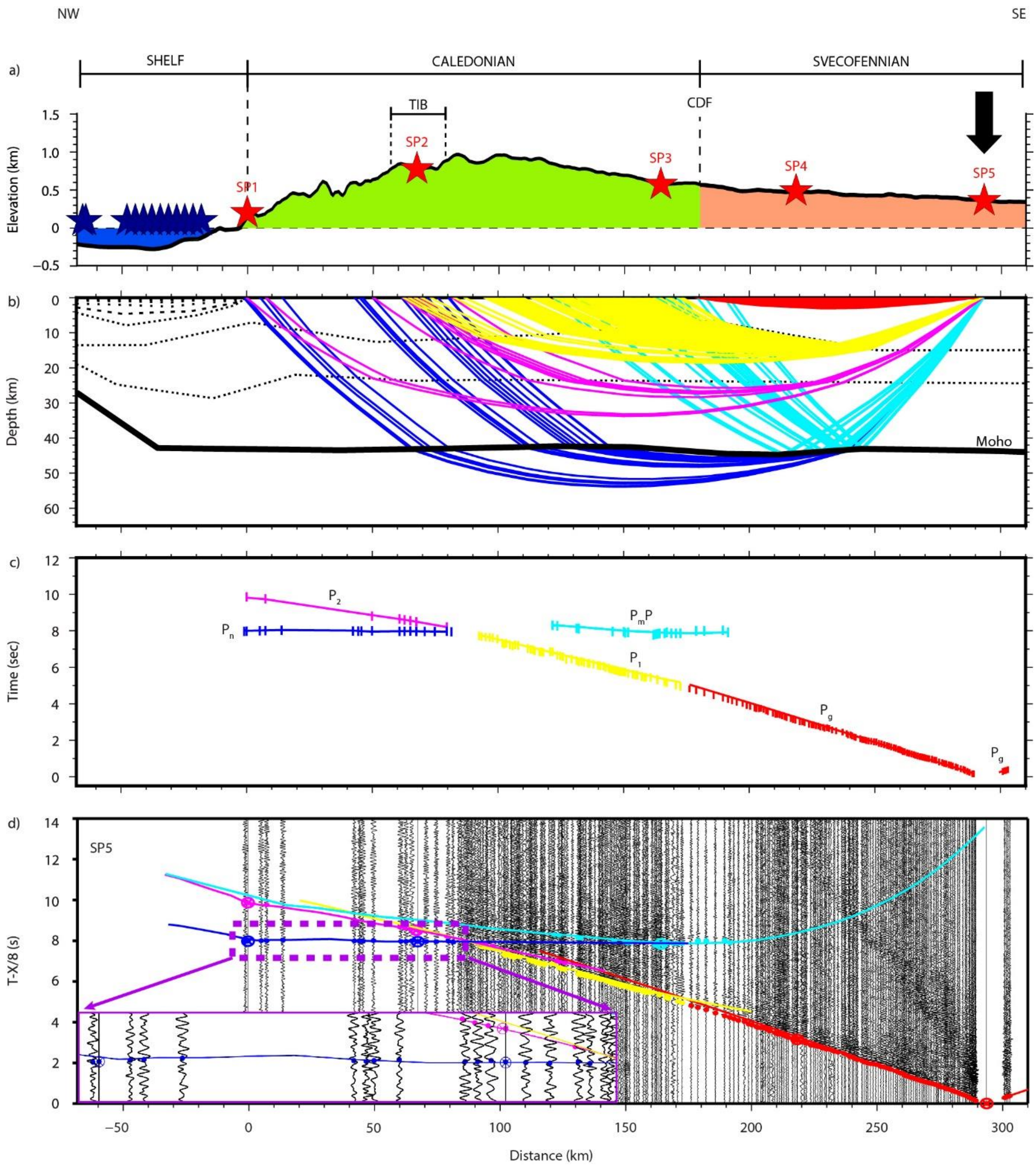

Supplementary Figure 9. Seismic travel time fit for SP5. As Supplementary Figure 4 for SP5 instead of SP1. Reciprocal arrival times for Pn are marked by purple crosses with circles (d) and in zoomed display for enhancing resolution of the Pn phase.

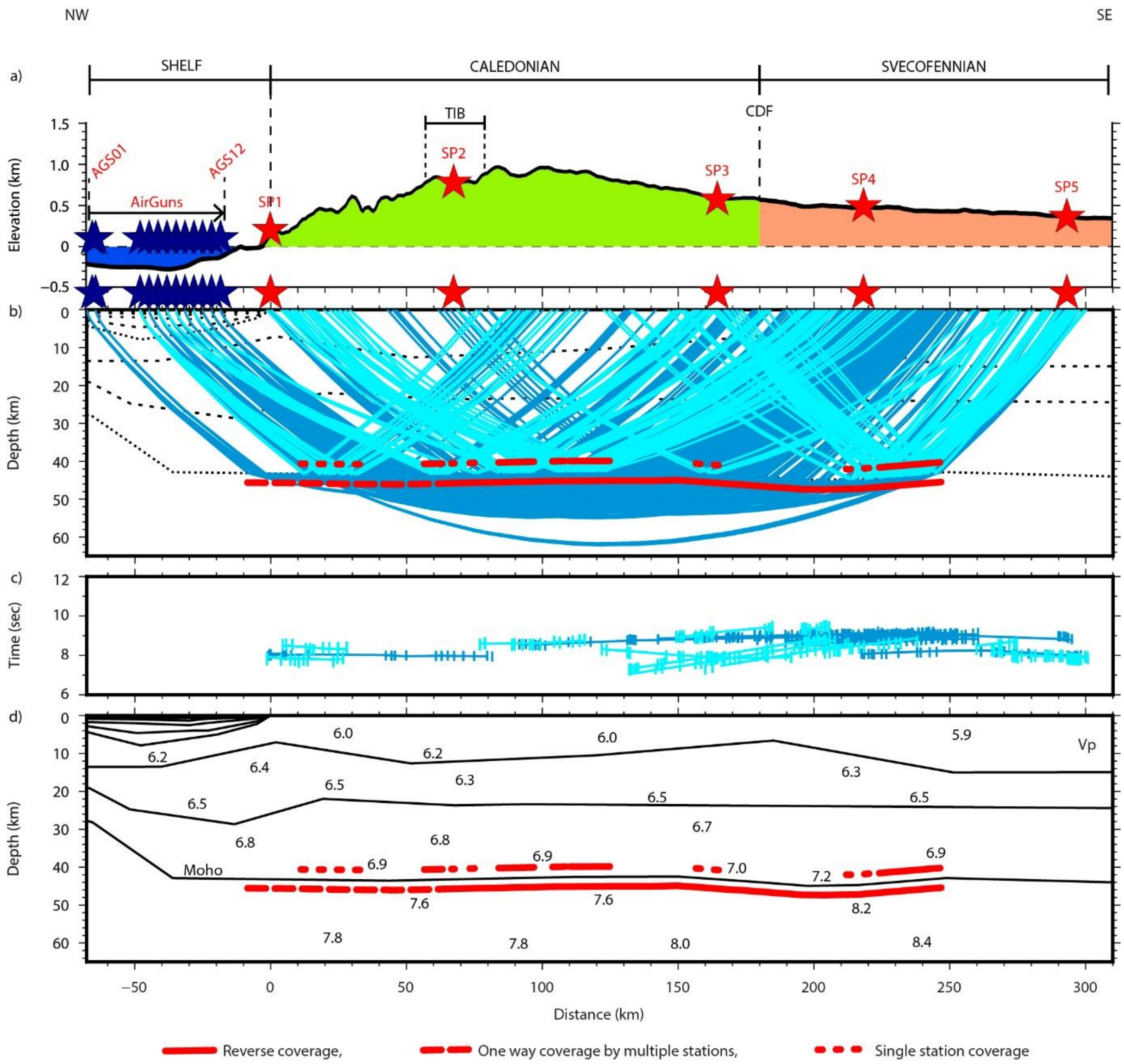

Supplementary Figure 10. Ray coverage of Moho by the PmP and Pn phases. As Supplementary Figure 2, illustrating rays (b) and arrival times (c) for the Moho phases PmP and Pn phases only. **b)** Turquoise solid lines show rays for PmP reflections from Moho, and light blue solid lines show rays for Pn refractions from Moho. **d)** Simplified velocity model with illustration of the coverage of Moho by the PmP and Pn phases as described in legend.

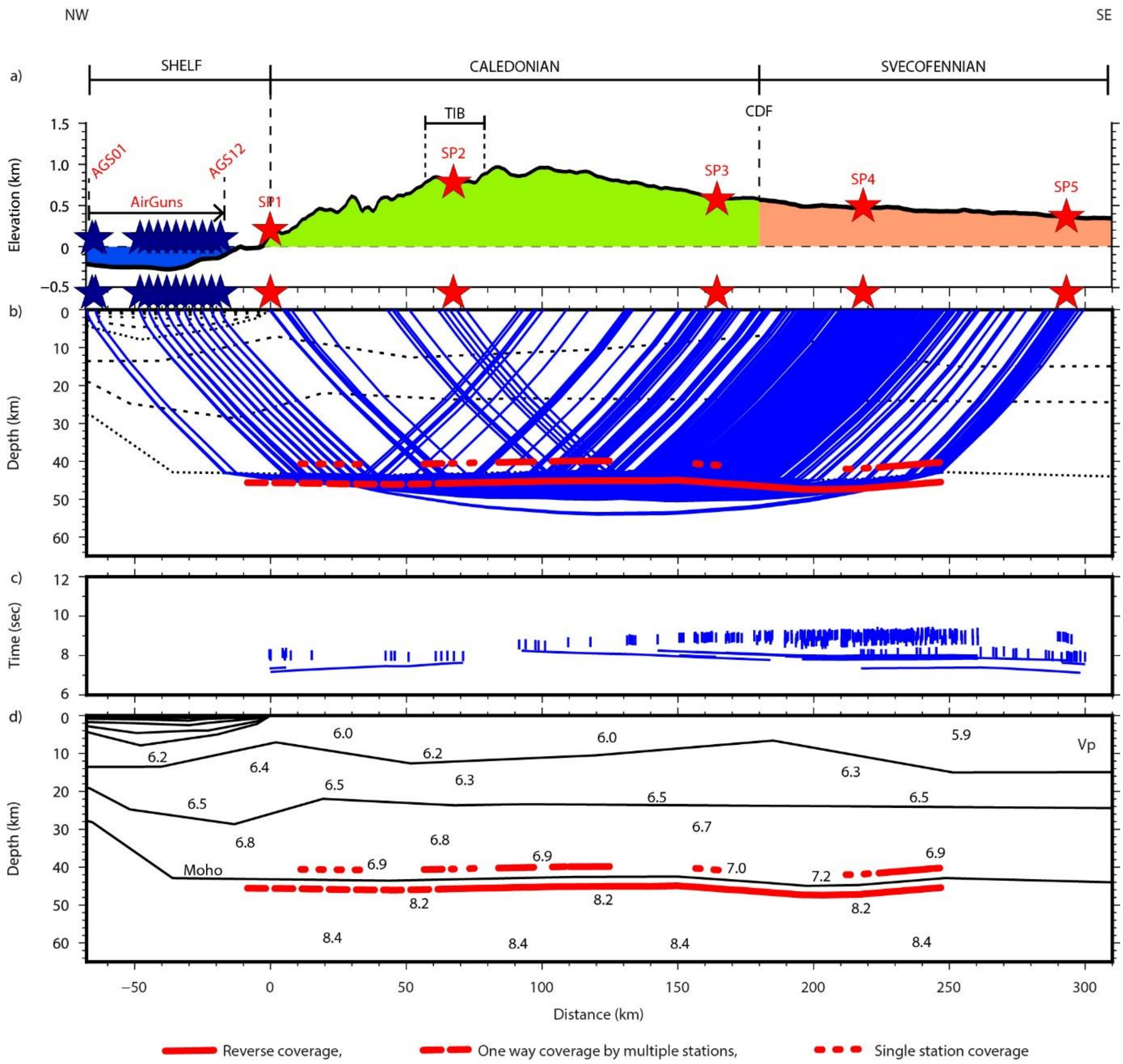

Supplementary Figure 11. Ray coverage of Moho by the Pn phases. As Supplementary Figure 10 for Pn instead of PmP and Pn. Sub-Moho velocity is constant to 8.2 km s^{-1}. Pn calculated times arrives early and do not fit on selected picks from the seismic section.

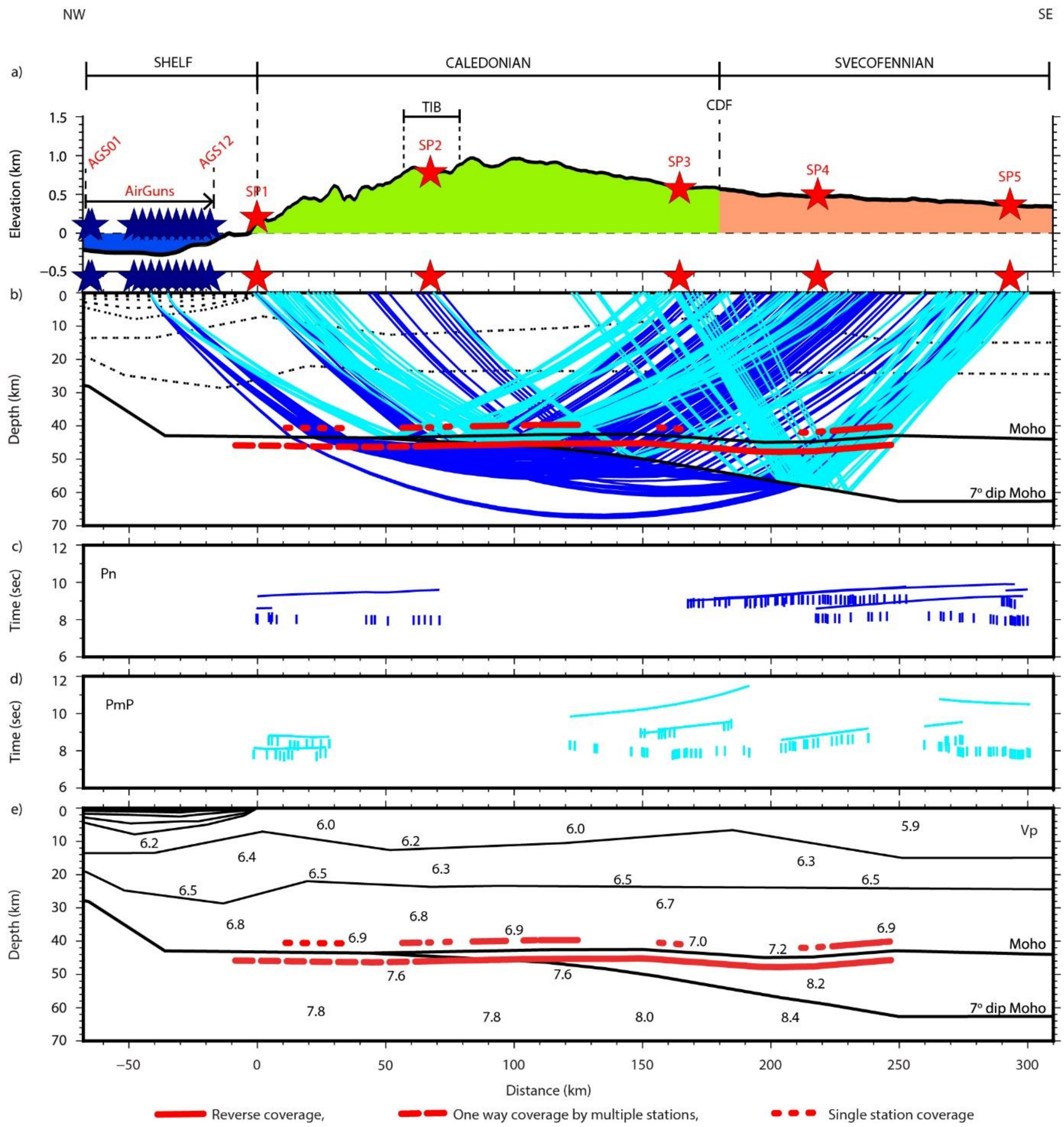

Supplementary Figure 12. Ray coverage of Moho by the PmP and Pn phases. As Supplementary Figure 10 except arrival times for 7^{o} dip Moho (c) and (d) for the Moho phases Pn and PmP phases only. e**)** Simplified velocity model with illustration of the coverage of 7^{o} dip Moho by the PmP and Pn phases.

Explanatory Note: Gravity Model Sensitivity Test

The density values in units C1, C2, S1 and S2 of the model are changed within possible ranges to observe how density variation affects the calculated gravity and hypsometry (Supplementary Figures 13b – 16b and Supplementary Figures 13a – 16a). We apply changes in steps of 0.050 g cm^{-3} for the density of units C1 and S1 (Supplementary Figures 13e and 15e) and 0.025 g cm^{-3} for units C2 and S2 (Supplementary Figures 14e and 16e).

The root mean square (RMS) difference between observed and calculated Bouguer anomaly is presented in Supplementary Figures 13d – 16d. Ideally, the minimum RMS values should represent the optimum density value for the objected unit. The lowest RMS value is provided by model test number 4 for unit C1 and unit C2 below the high topography (Supplementary Figures 13d and 14d) and model 5 for units S1 and S2 (Supplementary Figures 15d and 16d). We selected model 5 as our preferred model as we gave priority to fitting the calculated hypsometry rather than the Bouguer gravity anomaly, which fits within 23 mGal (Supplementary Figures 15d and 16d).

We also test the importance of the selected compensation depth of 120 km by calculating topography and Bouguer anomalies for variable density of C2 and S1 for compensation depths of 110 km (17) and 130 km (18). We apply similar changes in density steps of 0.025 g cm^{-3} (Supplementary Figures 17 and 18). We keep the same density in S1 and C2. The test shows that model 5 is stable for this 20 km variation of the compensation depth.

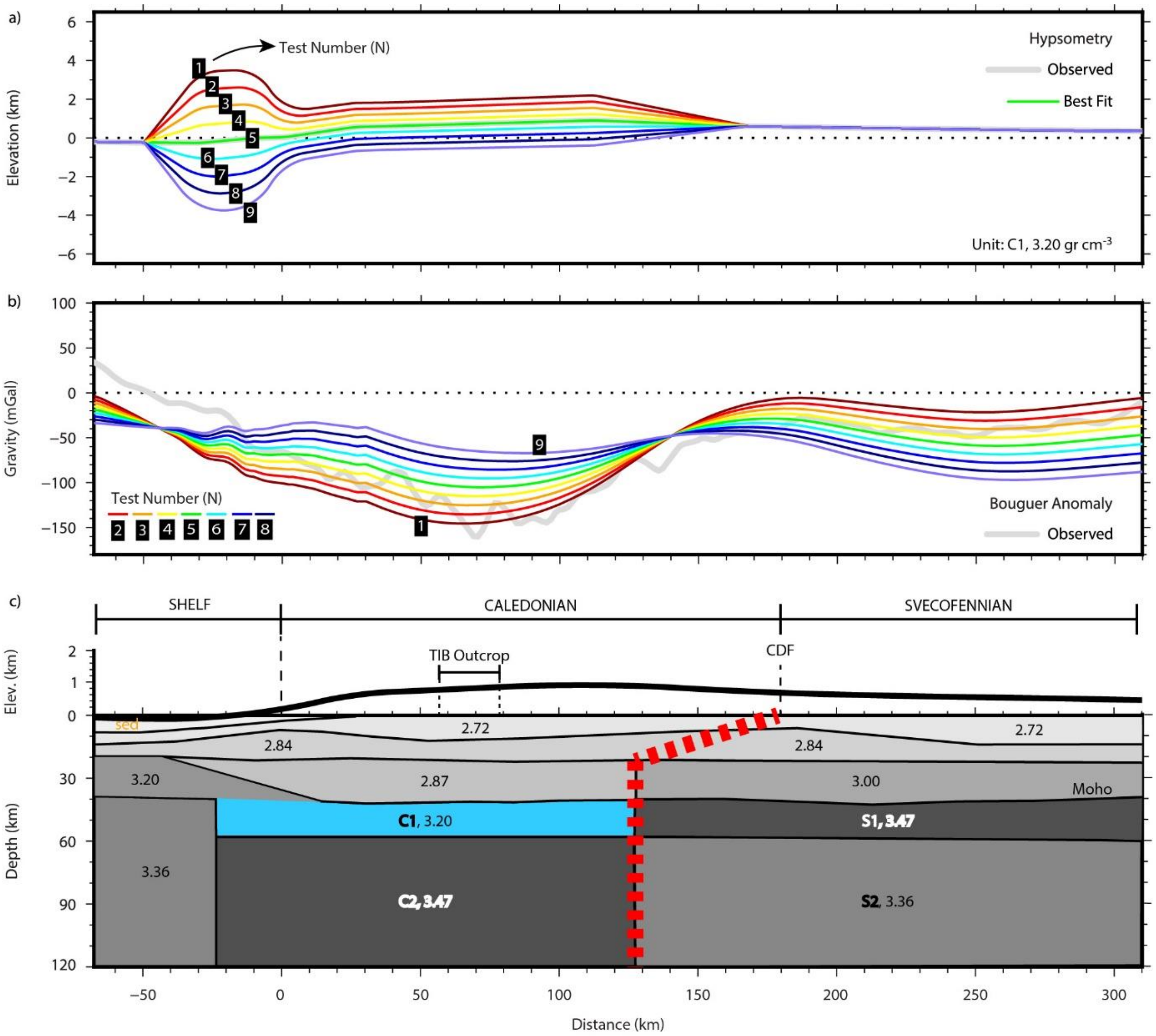

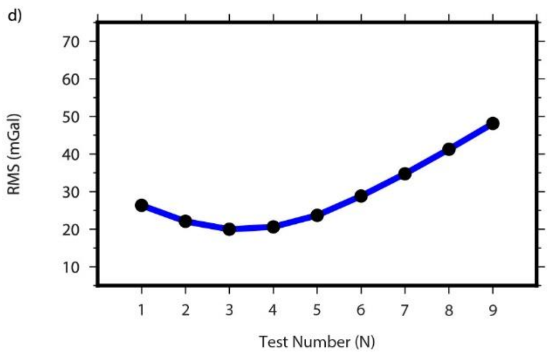

e)

N	Density (gr cm^{-3})	RMS (mGal)
1	3.000	26
2	3.050	22
3	3.100	20
4	3.150	21
5	**3.200**	**24**
6	3.250	29
7	3.300	34
8	3.350	41
9	3.400	48

Supplementary Figure 13. Gravity model sensitivity test for unit C1. a) Observed (thick grey line) and calculated (coloured lines from 1 to 9) hypsometry for variable density values given in (e). Densities of other units in the gravity model are held constant. **b)** Observed and calculated Bouguer anomalies for the same density variation. **c)** Gravity model with density units. CDF: Caledonian Deformation Front; TIB – Transscandinavian Igneous Belt. **d)** Root mean square (RMS) misfit between observed and calculated Bouguer anomalies versus test number. **e)** Table showing test number, density of unit C1 and RMS misfit of Bouguer anomaly.

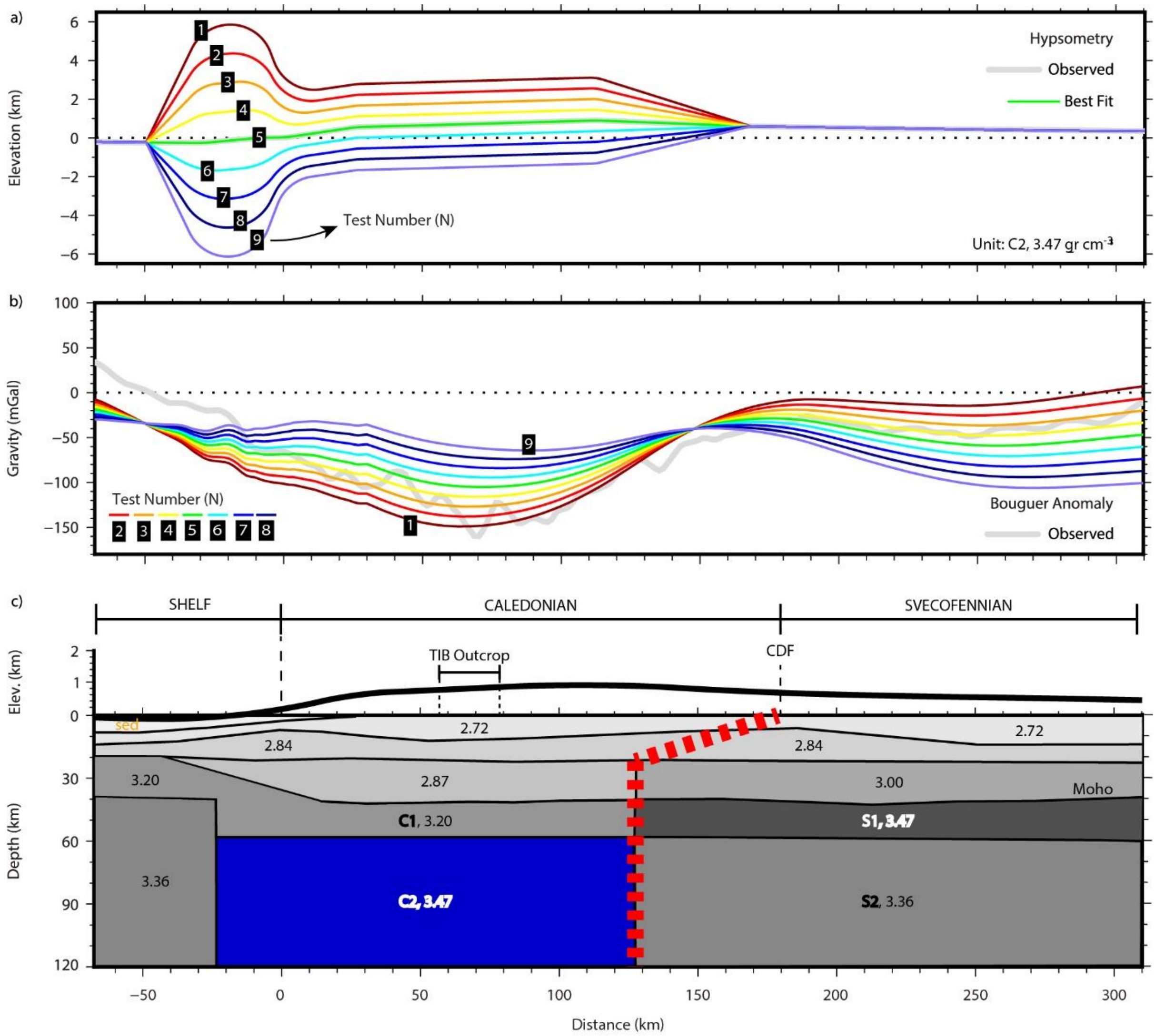

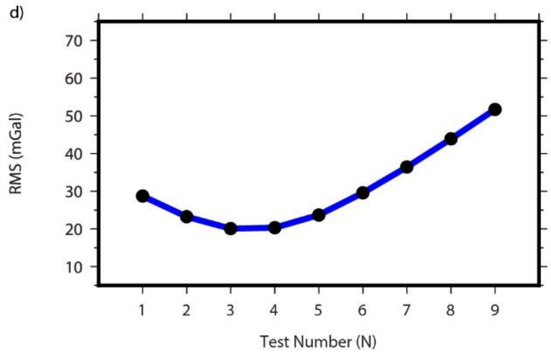

e)

N	Density (gr cm^{-3})	RMS (mGal)
1	3.370	29
2	3.395	23
3	3.420	20
4	3.445	21
5	**3.470**	**24**
6	3.495	30
7	3.520	36
8	3.545	44
9	3.570	52

Supplementary Figure 14. Gravity model sensitivity test for unit C2, cf. description in Supplementary Figure 10.

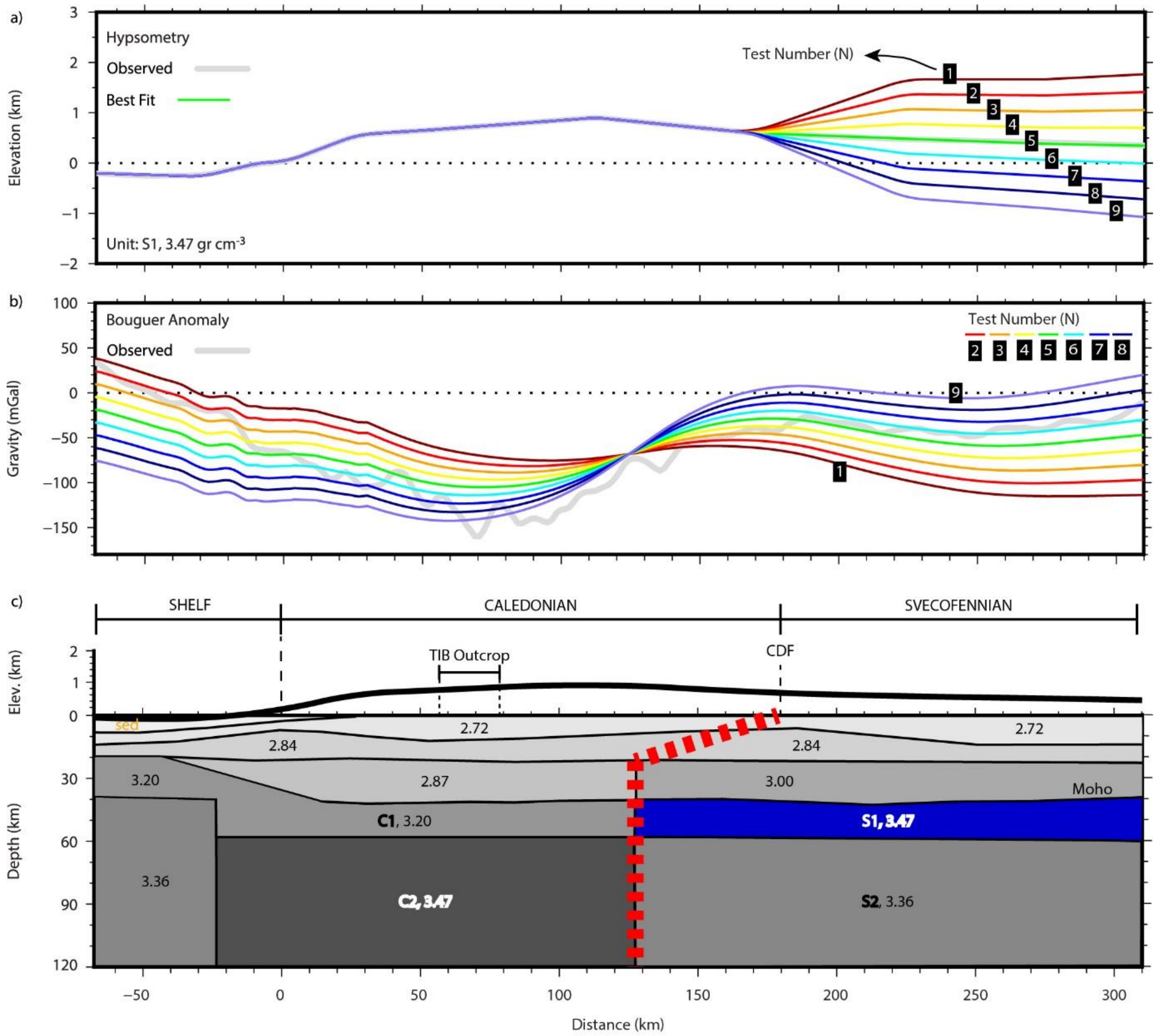

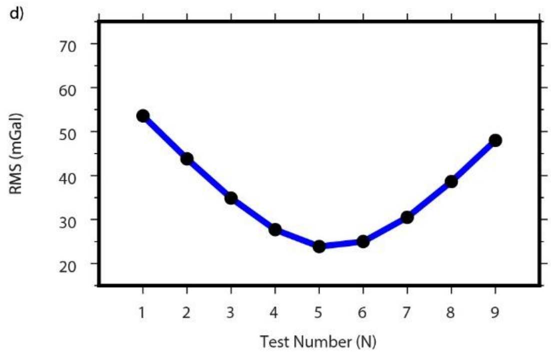

e)

N	Density (gr cm^{-3})	RMS (mGal)
1	3.270	54
2	3.320	44
3	3.370	35
4	3.420	28
5	**3.470**	**24**
6	3.520	25
7	3.570	31
8	3.620	39
9	3.670	48

Supplementary Figure 15. Gravity model sensitivity test for unit S1, cf. description in Supplementary Figure 10.

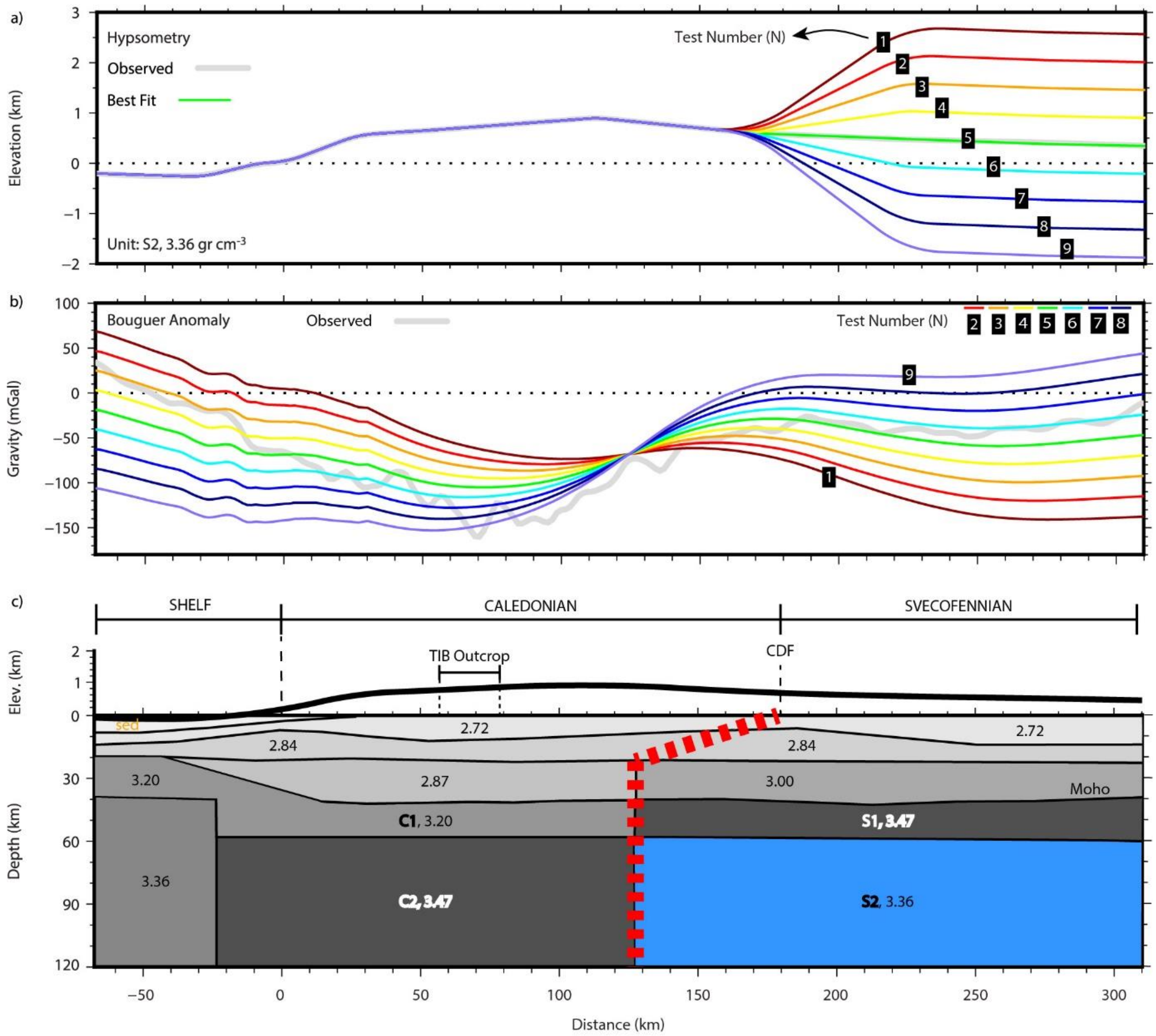

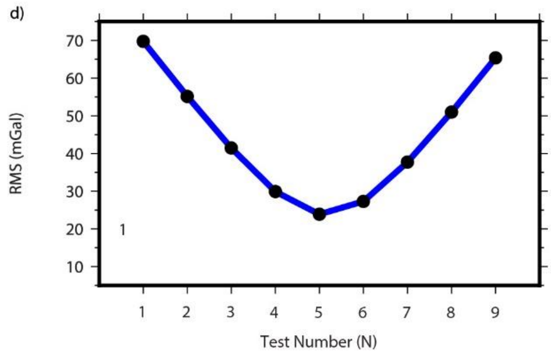

e)

N	Density (gr cm^{-3})	RMS (mGal)
1	3.260	70
2	3.285	55
3	3.310	41
4	3.335	30
5	**3.360**	**24**
6	3.385	27
7	3.410	38
8	3.435	51
9	3.460	65

Supplementary Figure 16. Gravity model sensitivity test for unit S2, cf. description in Supplementary Figure 10.

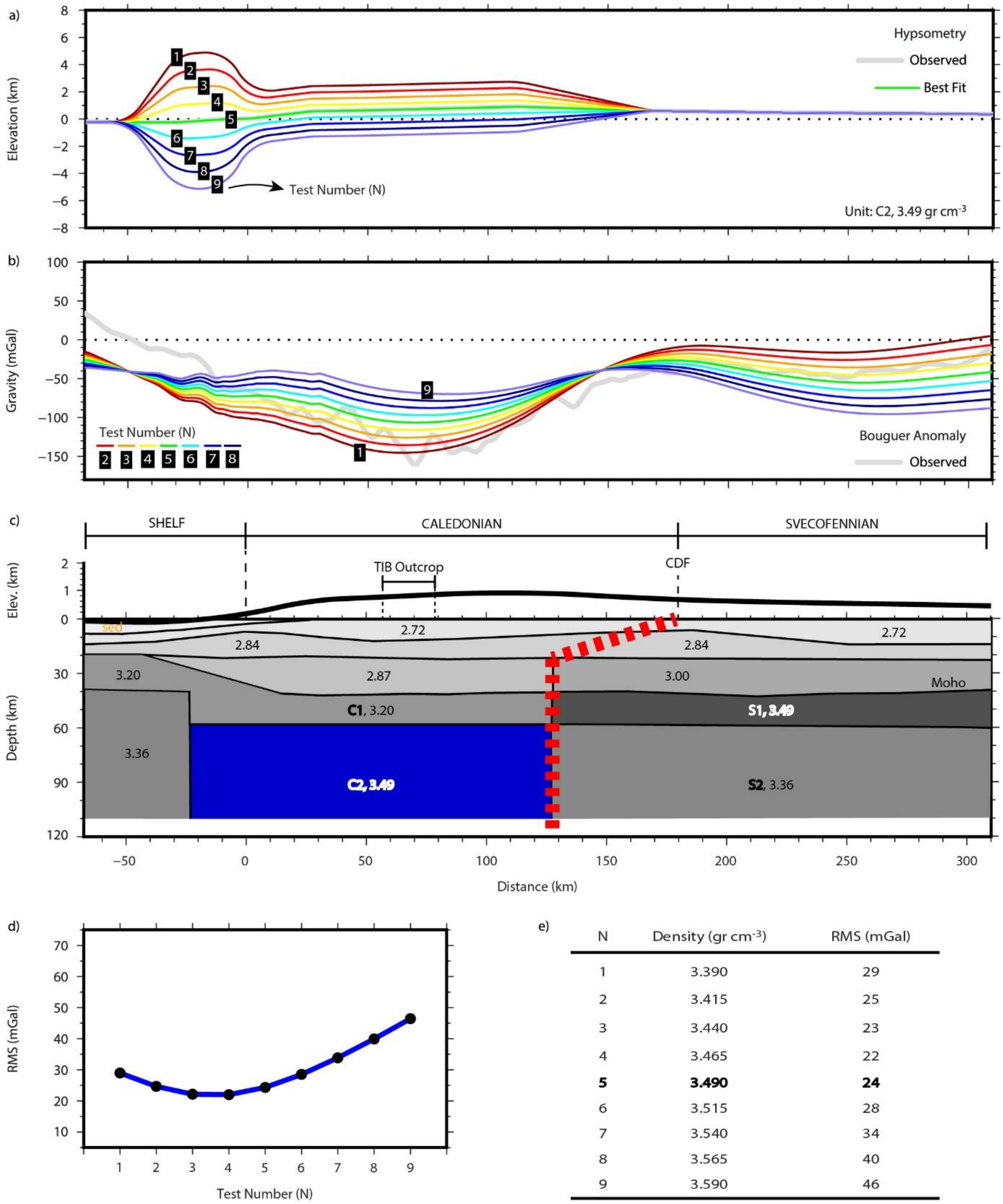

N	Density (gr cm^{-3})	RMS (mGal)
1	3.390	29
2	3.415	25
3	3.440	23
4	3.465	22
5	**3.490**	**24**
6	3.515	28
7	3.540	34
8	3.565	40
9	3.590	46

Supplementary Figure 17. Gravity model sensitivity test for unit for a compensation depth of 110 km instead of the selected 120 km, cf. description in Supplementary Figure 10.

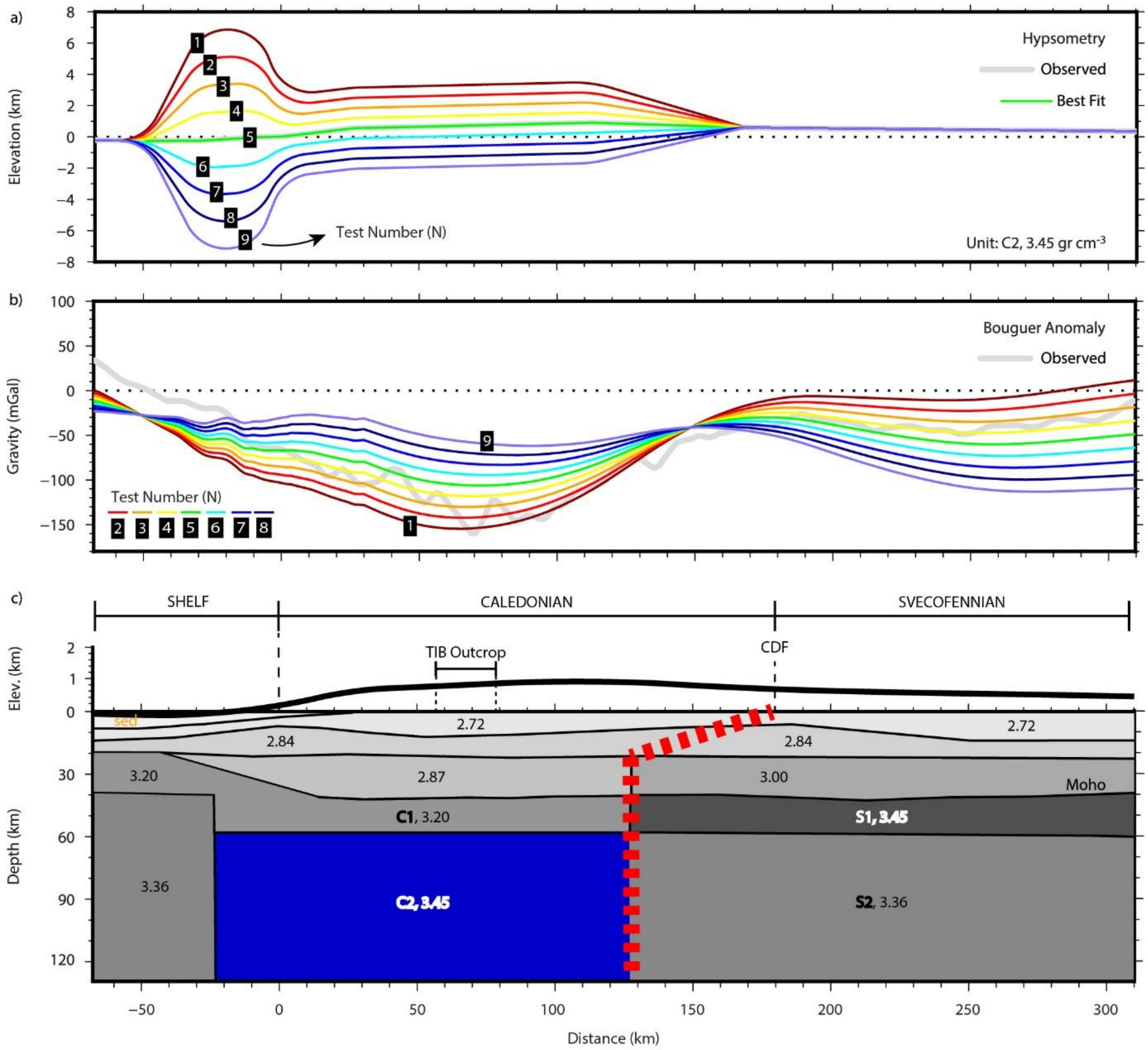

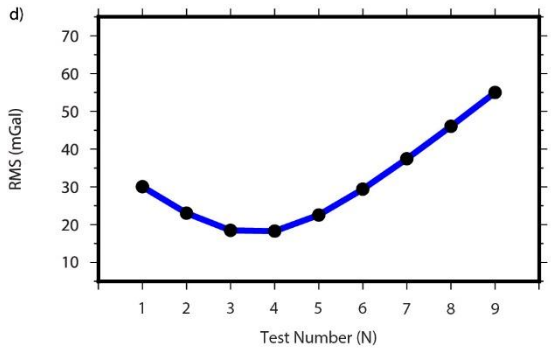

e)

N	Density (gr cm^{-3})	RMS (mGal)
1	3.350	30
2	3.375	23
3	3.400	19
4	3.425	18
5	**3.450**	**23**
6	3.475	29
7	3.500	38
8	3.525	46
9	3.550	55

Supplementary Figure 18. Gravity model sensitivity test for unit for a compensation depth of 130 km instead of the selected 120 km, cf. description in Supplementary Figure 10.

Supplementary Table 1. Seismic station parameters for data acquisition.

Number of stations	Recorder	Sampling rate [ms]
170	Texan	4
102	Sercel	6

Supplementary Table 2. Shot parameters for data acquisition.

Shot points Number	Latitude(°)	Longitude(°)	Altitude(m)	Charge size
AGS01	67.5876	13.0157	0	18 x 22 ℓ
AGS02	67.5704	13.0788	0	18 x 22 ℓ
AGS03	67.4839	13.3925	0	18 x 22 ℓ
AGS04	67.4665	13.4549	0	18 x 22 ℓ
AGS05	67.4492	13.5174	0	18 x 22 ℓ
AGS06	67.4317	13.5796	0	18 x 22 ℓ
AGS07	67.4143	13.6419	0	18 x 22 ℓ
AGS08	67.3968	13.7039	0	18 x 22 ℓ
AGS09	67.3793	13.7659	0	18 x 22 ℓ
AGS10	67.3618	13.8278	0	18 x 22 ℓ
AGS11	67.3443	13.8897	0	18 x 22 ℓ
AGS12	67.3270	13.9520	0	18 x 22 ℓ
SP1	67.1373	14.1251	45	400 kg
SP2	66.8049	15.4244	158	200 kg
SP3	66.2887	17.1822	487	200 kg
SP4	66.0685	18.2765	500	200 kg
SP5	65.5812	19.4484	434	400 kg

Supplementary Table 3. Statistical parameters of seismic P-wave modelling for all shots.

Phase Number	Total number of picks	The number of picks for modelling	Uncertainty(ms)	t_{RMS}(ms)	χ^2
P_g	610	600	75	0.094	1.561
P_1	446	446	75	0.070	0.874
$P_{c1}P$	80	80	100	0.074	0.562
P_2	97	87	75	0.041	0.166
$P_{c2}P$	74	74	100	0.071	0.513
P_mP	128	128	100	0.084	0.708
P_n	341	338	100	0.049	0.240
Total	1776	1753		0.076	0.908

Supplementary Table 4. Statistical parameters of seismic P-wave modelling for onshore explosive sources.

Phase Number	Total number of picks	The number of picks for modelling	Uncertainty(ms)	t_{RMS}(ms)	χ^2
P_g	586	577	75	0.095	1.596
P_1	195	195	75	0.082	1.215
$P_{c1}P$	77	77	100	0.076	0.581
P_2	41	37	75	0.035	0.124
$P_{c2}P$	19	19	100	0.122	1.561
P_mP	89	89	100	0.089	0.807
P_n	54	53	100	0.048	0.239

Total	1061	1047		0.088	1.257

Supplementary Table 5. Statistical parameters of seismic P-wave modelling for airgun shots.

Phase Number	Total number of picks	The number of picks for modelling	Uncertainty(ms)	t_{RMS}(ms)	χ^2
P_g	24	23	75	0.062	0.706
P_1	251	249	75	0.059	0.616
$P_{c1}P$	3	3	100	0.029	0.122
P_2	56	54	75	0.045	0.202
$P_{c2}P$	55	55	100	0.041	0.171
P_mP	39	39	100	0.069	0.495
P_n	287	287	100	0.049	0.239
Total	715	710		0.053	0.389